THE LOAD CAPACITY AND STIFFNESS OF THE AXIAL PERMANENT MAGNET BEARINGS

Matti J. Antila
Laboratory of Electromechanics, Helsinki, Finland

ABSTRACT

This paper deals with the load capacity and stiffness of axial permanent magnet bearings and their influence on possible applications. We have studied the influence of the geometric parameters of a ring shaped axial bearing on the load capacity and stiffness. We have used the analytical solution of the flux density and calculated the values numerically. Characteristics of both attractive and repulsive bearing types have been analysed

INTRODUCTION

Active magnetic bearings are a complex and expensive alternative to conventional roller and liquid bearings. They demand an external power source and active control. Problems with active magnetic bearings could be avoided by using permanent magnet bearings. They don't need an external power source, are reliable and have a long lifetime. However, an object can only be levitated freely in a permanent magnet field if the relative permeability of the object is less than one [1]. So, permanent magnet bearing can only be utilised as a part of the suspension system. For example, a combination of radial gas bearings and axial permanent magnet bearings would have some potential applications. The main problems of permanent magnet bearings are the low stiffness and sensitivity to external perturbations. These problems restrict applications with small air gabs and heavy weight rotors [2].

Forces acting in permanent magnet bearings have been previously calculated neglecting the curvature [3,4], which is a valid assumption if the curvature is large compared to the height and width of the permanent magnet ring. Force calculation combining permanent magnets and electromagnets have also been carried out [5]. In this paper a special case of the three dimension problem (cylindrical symmetry) is calculated. Due to the symmetry, the problem is reduced to two dimensions and an analytical solution to the flux density can be found.

CALCULATION OF THE FLUX DENSITY

The flux density $\bar{B}$ of one permanent magnet ring can be calculated from the vector potential $\bar{A}$

$$\bar{B} = \nabla \times \bar{A}. \tag{1}$$

In the case of a permanent magnet with magnetisation $\bar{M}$ the vector potential is

$$\bar{A} = -\frac{\mu_0}{4\pi}\int \frac{\nabla \times \bar{M}}{r} dv, \tag{2}$$

where μ_0 is permeability of vacuum and the integration goes over the volume of the permanent magnet.

Axial magnetisation

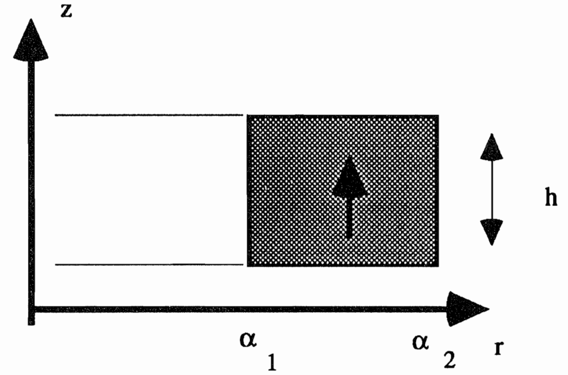

FIGURE 1: The geometry of a permanent magnet ring with axial magnetisation.

The solution of the flux density in radial and axial directions for a ring shaped permanent magnet with axial magnetisation (Figure 1) is

$$\begin{aligned} B_r(r,z) &= -M_0 F_r(r,z) \\ B_z(r,z) &= -M_0 F_z(r,z) \end{aligned} \tag{3}$$

$$F_r(r,z) = \int_0^h [f_r(\alpha_1,r,z-h) - f_r(\alpha_2,r,z-h)]dh$$
$$F_z(r,z) = \int_0^h [f_z(\alpha_1,r,z-h) - f_z(\alpha_2,r,z-h)]dh, \tag{4}$$

where M_0 is magnetisation strength, h is the height of the permanent magnet ring, α_1 is the inner radius of the permanent magnet ring and α_2 is the outer radius of the permanent magnet ring.

$$f_r(\alpha,r,z) = \frac{1}{2\pi}\frac{z}{r\sqrt{(\alpha+r)^2+z^2}} \times \left[\frac{\alpha^2+r^2+z^2}{(\alpha-r)^2+z^2}E(k) - K(k)\right]$$
$$f_z(\alpha,r,z) = \frac{1}{2\pi}\frac{1}{\sqrt{(\alpha+r)^2+z^2}} \times \left[\frac{\alpha^2-r^2-z^2}{(\alpha-r)^2+z^2}E(k) + K(k)\right]$$
$$K(k) = \int_0^{\pi/2} \frac{d\theta}{\sqrt{1-k^2\sin^2\theta}} \tag{5}$$
$$E(k) = \int_0^{\pi/2} \sqrt{1-k^2\sin^2\theta}\,d\theta$$
$$k^2 = \frac{4\alpha r}{(\alpha+r)^2+z^2},$$

where $K(k)$ and $E(k)$ are the elliptic integrals of the first and second kind.

Radial magnetisation

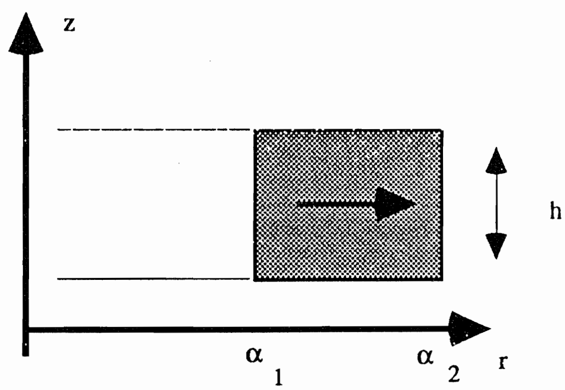

FIGURE 2: The geometry of a permanent magnet ring with radial magnetisation.

The solution of the flux density in radial and axial directions for a ring shaped permanent magnet with radial magnetisation (figure 2) is

$$B_r(r,z) = -M_0 G_r(r,z)$$
$$B_z(r,z) = -M_0 G_z(r,z) \tag{6}$$

$$G_r(r,z) = \int_{\alpha_1}^{\alpha_2} [f_r(a,r,z-h) - f_r(a,r,z)]da$$
$$G_z(r,z) = \int_{\alpha_1}^{\alpha_2} [f_z(a,r,z-h) - f_z(a,r,z)]da, \tag{7}$$

where the symbols are the same as in formula (4).

FORCE CALCULATION

The axial force or load capacity between permanent magnet rings is calculated as follows.

$$F_z = \int_S (T_{zr}n_r + T_{\theta}n_{\theta} + T_{zz}n_z)dS$$
$$F_z = \frac{1}{\mu_0}\int_S (B_r B_z n_r + \frac{B_z^2 - B_r^2}{2}n_z)dS \tag{8}$$

where T_{zr}, $T_{z\theta}$, T_{zz} are components of Maxwell's stress tensor and n_r, n_θ and n_z are the components of unit vector normal to the surface S. In case of cylindrical symmetry $n_\theta = 0$, so the force can be calculated from integral (8), where surface S bounds the volume of the other permanent magnet ring.

Repulsive axial permanent magnet bearing

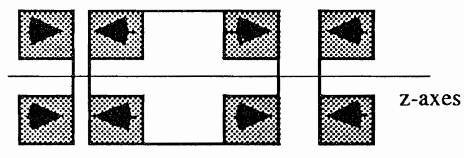

FIGURE 3: A repulsive axial permanent magnet bearing system.

In case of two repulsive magnets the surface (Figure 3) can be taken as normal to z-axes so the integral is simplified.

$$F_z = \frac{1}{2\mu_0}\int_0^\infty 2\pi r(B_z^2 - B_r^2)dr \tag{9}$$

The axial force of a repulsive axial magnetic bearing is calculated with three values of height h and width b (6, 12 and 18 mm). The outer radius of the permanent magnet ring is 20 mm and magnetisation strength is 0.83 T. In Figure 4 axial force F_Z is shown for the nominal air gap of 6 mm, where the forces from the repulsive permanent magnet rings are equal but opposite. The load capacity is larger with larger height and width of permanent magnet rings.

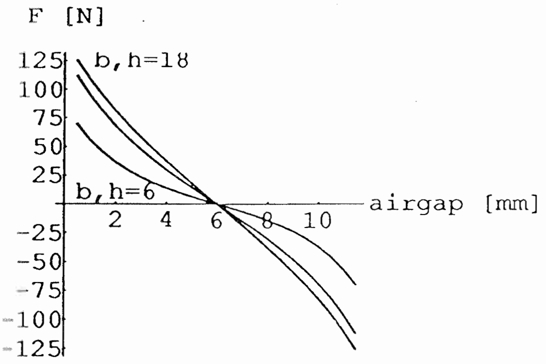

FIGURE 4: The axial force of a repulsive axial permanent magnet bearing (nominal air gap 6 mm).

In Figure 5 the same configuration as in Figure 4 is shown for the nominal air gap of 3 mm. The axial force with larger air gap is larger due to the opposite forces of the repulsive permanent magnet rings.

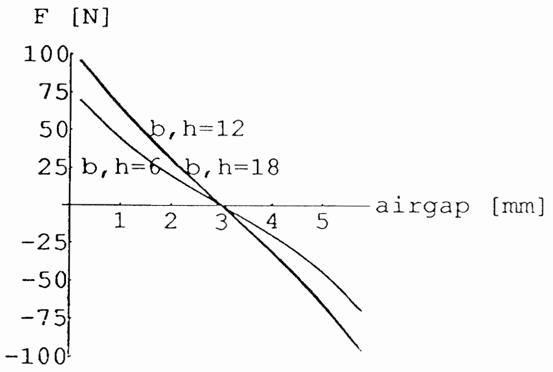

FIGURE 5: The axial force of a repulsive axial permanent magnet bearing (nominal air gap 3 mm).

The stiffness C of an axial bearing is the derivative of the axial force with respect to the deviation e from the nominal position. In Figures 6 and 7 the stiffness of a repulsive axial bearing is calculated with the same parameters as the load capacities in Figures 4 and 5 with the nominal air gabs of 6 mm and 3 mm. With the larger nominal air gap the stiffness in the neighbourhood of the nominal position is smaller than the stiffness with the smaller nominal air gap. Also the larger the height and width of the permanent magnet rings the larger the stiffness is.

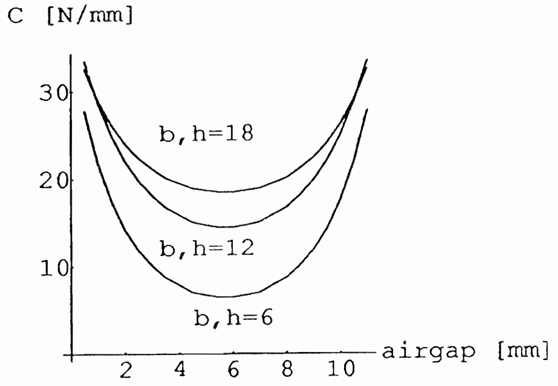

FIGURE 6: The stiffness of a repulsive axial permanent magnet bearing (nominal air gap 6 mm).

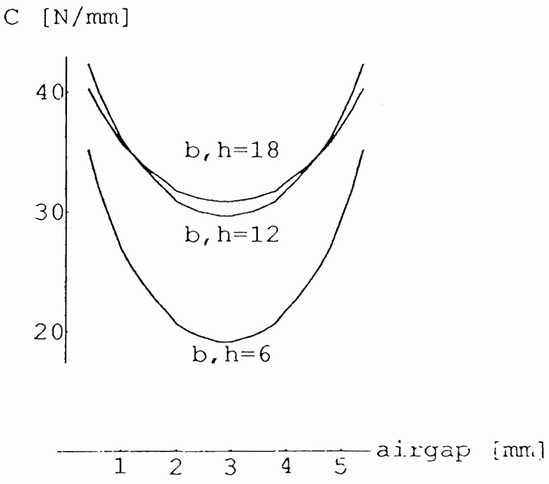

FIGURE 7: The stiffness of a repulsive axial permanent magnet bearing (nominal air gap 3 mm).

Attractive axial permanent magnet bearing

In case of two concentric permanent magnet rings with radial magnetisation (Figure 8) the integration surface can be taken as normal to r-axes so the integral is simplified.

$$F_z = \frac{1}{\mu_0} \int_{-\infty}^{\infty} 2\pi r B_z B_r dz \qquad (10)$$

where r is the radius of the integration surface.

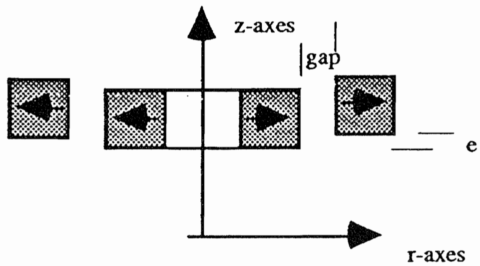

FIGURE 8: An attractive axial permanent magnet bearing.

In Figure 9 the axial force of an attractive permanent magnet bearing is shown with three values of height h and width b. The outer radius of the inner permanent magnet ring is 20 mm and gap 1 mm. The force is calculated as a function of the deviation e from the nominal position, where the permanent magnet rings are exactly concentric. The axial force or load capacity increases with the increasing deviation until a maximum load capacity is met, then the load capacity diminishes with the increasing deviation.

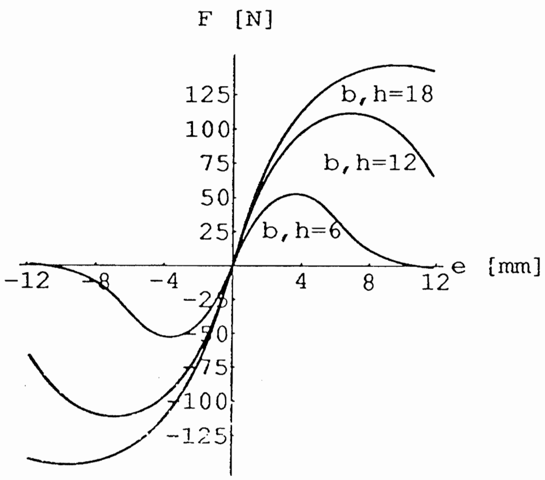

FIGURE 9: The axial force of an attractive axial permanent magnet bearing.

In Figure 10 the stiffness of an attractive axial permanent magnetic bearing is shown with the same parameters as the load capacity in Figure 9. The attractive axial bearing is found to be very stiff in the neighbourhood of the nominal position while the stiffness diminishes at larger deviations. In Figures 6 and 10 the characteristic difference of the repulsive and attractive permanent magnet bearings is clearly seen.

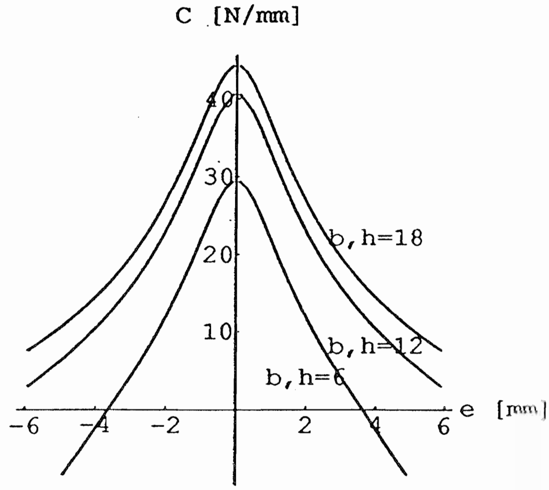

FIGURE 10: Stiffness of attractive axial permanent magnet bearing.

The effect of the gap between the inner and outer concentric permanent magnet rings (Figure 8) on the load capacity is shown in Figure 11. Height h and width b are 12 mm. Obviously, the axial force is larger with smaller gaps.

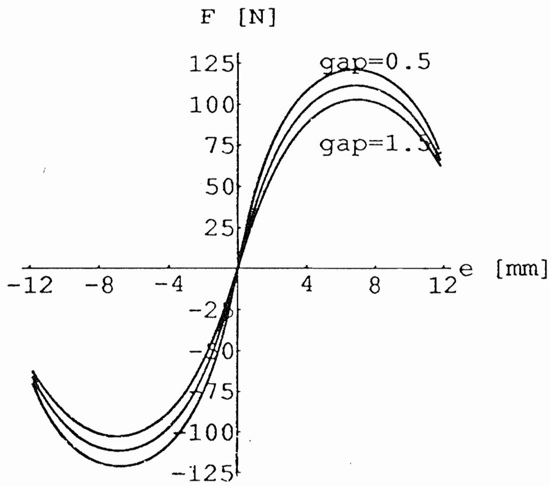

FIGURE 11. The effect of the gap on the axial force.

CONCLUSION

The load capacity and stiffness of axial permanent magnet bearings are calculated from the analytical solution numerically. The load capacities are found to be reasonable, but the low stiffness at large air gabs in repulsive-type bearings restricts their usage. Attractivetype bearings are found to be stiffer in the neighbourhood of the nominal position. Anyhow, the total energy involved in spring motion from the nominal position to the extreme position is still quite low for both types of bearings. This total energy can be interpreted as the total damping capacity of a bearing and in that sense it describes the sensitivity of the bearing system on external perturbations.

REFERENCES

1. Brauenbek W., Freischwebende Körper im elektrischen und magnetischen Feld, Zeitschrift für Physik, Vol 112, pp. 753-763, 1939.
2. Boden K., Fremerey J.K., Industrial realization of the "System KFA-Julich" permanent magnet bearing lines, Proceedings of MAG 1992 Magnetic Bearings, Magnetic Drives and Dry Gas Seals Conference & Exhibition, Virginia, USA, pp. 43-60, 1992.
3. Yonnet J.-P., Analytical calculation of magnetic bearings, Proceedings of the 5th International Workshop on RE-Co Permanent Magnets, Roanake VA, USA, pp. 199-216, 1981.
4. Sobottka G., Hubner K.-D., Dauermagnetische Radiallager und Axiallager: Entwicklungsstand und Tendenz, Maschinenmarkt, Vol. 87, No. 5, pp. 55-58, Wurzburg, 1981.
5. Nagaya K., Arai N., Analysis of a permanent magnet levitation actuator with electromagnetic control, Transaction of the ASME, Vol. 113, pp. 472-478, September 1991.